

Characterization of the boundary layer at Dome C (East Antarctica)

during the OPALE summer campaign

Gallée, H.¹, S. Preunkert¹, S. Argentini², M. M. Frey³, C. Genthon¹, B. Jourdain¹, I. Pietroni², G. Casasanta², H. Barral¹, E. Vignon¹, C. Amory¹ and M. Legrand¹

5 (1) CNRS/UJF-Grenoble 1, Laboratoire de Glaciologie et Géophysique de l'Environnement, France

(2) Istituto di Scienze dell' Atmosfera e del Clima (ISAC) - CNR , Italy

(3) British Antarctic Survey, Natural Environment Research Council, Cambridge, UK

Abstract

The regional climate model MAR (Modèle Atmosphérique Régional) was run for the region of
10 Dome C located on the East Antarctic plateau, during Antarctic summer 2011 - 2012, in order to
refine our understanding of meteorological conditions during the tropospheric chemistry
campaign OPALE. A very high vertical resolution is set up in the lower troposphere, with a grid
spacing of roughly 2 m. Model output is compared with temperatures and winds observed near
the surface and from a 45 m high tower as well as sodar and radiation data. MAR is generally in
15 very good agreement with the observations but sometimes underestimates cloud formation,
leading to an underestimation of the simulated downward long-wave radiation. Absorbed short-
wave radiation may also be slightly overestimated due to an underestimation of the snow albedo
and this influences the surface energy budget and atmospheric turbulence. Nevertheless the
model provides sufficiently [reliable information about surface turbulent fluxes, vertical profiles of](#)
20 [vertical diffusion coefficients and boundary layer height](#) when discussing the representativeness
of chemical measurements made nearby the ground surface during field campaigns conducted at

Concordia station located at Dome C (3233 m above sea level).

1. Introduction

The aim of this paper is to **evaluate** MAR (Modèle Atmosphérique Régional) simulations during the
25 OPALE campaign at Dome C in austral summer 2011 – 2012 (from late November 2011 to mid-
January 2012), to support the interpretation of observations of tropospheric chemistry. A
particular purpose is to characterize the behaviour and the vertical structure of the boundary layer
at Dome C during this period.

A similar study has been carried out previously above the East Antarctic plateau, based on summer
30 time observations at Kohnen station in Dronning Maud land, albeit only with a more simplistic 1-D
model (Van As et al., 2006).

Dome C is an area where observation and modelling of the boundary layer has already been
performed due to its particular location (Swain and Gallée, 2006, Sadibekova et al., 2006, King et
al., 2006, Gallée and Gorodetskaya, 2010, Genthon et al., 2010, 2013, Brun et al., 2011, Lascaux et
35 al., 2011, Argentini et al. 2013, Pietroni et al. , 2014). Furthermore , Dome C was recently selected
as the test site for the next Gewex Atmospheric Boundary Layer Studies (GABLS4) model
intercomparison (see <http://www.cnrm.meteo.fr/aladin/meshtml/GABLS4/GABLS4.html>). In spite of its
remote location Concordia station, operated year-round, is logistically well supported due to a
number of reasons. Dome C had been chosen as part of the EPICA project for drilling the ice core
40 with the longest climate chronology ever recorded, allowing to study the climate of the last eight
glacial cycles (EPICA community members, 2004). The EPICA project initiated extensive
meteorological observations at Dome C, in order to establish, among others, the relationship
between local and global climate. Therefore setting up a regional model at the Dome C drilling site
enables (i) to assimilate large scale meteorological conditions and (ii) to simulate local atmospheric

45 conditions, which contributes to establishing this relationship. The good management of logistics between the Concordia station and the Antarctic coast (Terre Adélie) and the low optical turbulence at Dome C also promoted the site for astronomical observations (see e.g., Swain and Gallée, 2006, Sadibekova et al., 2006). The main characteristic of meteorological conditions at Dome C is that turbulent conditions in the near-surface atmosphere are only effective in a rather
50 shallow layer, especially during night-time (Pietroni et al. , 2014). [During day-time the sensible heat fluxes are much larger than the latent heat fluxes, because of low temperatures and subsequently very low atmospheric moisture content \(King et al., 2006\). Consequently the conditions for development of a well mixed layer during daytime are optimal, in contrast to the situation in coastal Antarctica such as Halley station \(King et al., 2006\). This means that the simulation of](#)
55 [summer case studies at Dome C will be very useful in validating the turbulence scheme of atmospheric models.](#) Sodar and sonic anemometer measurements were done at the Concordia station to monitor the turbulent structure of the planetary boundary layer (PBL) in connection with the temperature inversion and estimate the PBL height in the frame of the ABLCLIMAT (Atmospheric Boundary Layer Climate) project (Argentini et al. 2013).

60 The 45 m high tower built up at Concordia is also a very useful tool for observing such conditions (Genthon et al., 2010, 2013). Short-term meteorological simulations have already been done over Dome C with a coupled atmosphere – snow model, focusing on the behaviour of the snow model (Brun et al., 2011). Long term simulations of the Antarctic climate have also been done, with a focus on their behaviour at Dome C. Swain and Gallée (2006) and Lascaux et al. (2011) used
65 respectively the limited area models MAR (without any reinitialisation of meteorological variables) and Meso-NH to compare the optical properties of the atmosphere at Dome C with those of other potential Antarctic sites for astronomical observations using a large telescope. Gallée and Gorodetskaya (2010) validated MAR for winter conditions, emphasizing the difficulty to accurately

simulate the downward long-wave radiation and proposing to include the influence of small
70 airborne snow particles in the parameterization of the radiation transfer. MAR has also been used
for providing information on the atmospheric turbulence at Dome C in summer, which appears to
very significantly control the vertical flux and concentration profiles of numerous atmospheric
chemical species (Legrand et al., 2009, Kerbrat et al., 2012; Dommergue et al., 2012, Frey et al.,
2013). Finally two years of observations at the Dome C tower were used to compare a long-term
75 simulation of MAR with ECMWF analyses, showing the interest to represent the atmosphere with a
fine vertical resolution (Genthon et al., 2013). Here we go a step further by [evaluating in detail](#) the
model for summer conditions during the OPALE campaign.

[The general motivation of the present research is to provide tools from a meteorological point of
view for future campaigns dedicated to investigate the chemical composition of the Antarctic
80 boundary layer above the East Antarctic plateau. Thus, the first objective of this paper is to
evaluate a meteorological model that is capable of simulating transport and that can be coupled to
a chemical routine.](#)

[The second objective of the paper is to provide key physical parameters of the atmospheric
boundary layer for the interpretation of data gained during the OPALE campaign as detailed in
85 companion papers \(see Legrand et al., 2014; Kukui et al., 2014; Frey et al., 2014, and Preunkert et
al., 2014\). Transport processes are not considered during the 2011-2012 OPALE campaign and we
will focus on situations characterized by an atmospheric circulation localized over the Antarctic
plateau, where chemical properties of the air are rather homogeneous from one point to another.
This means that from a meteorological point of view atmospheric turbulence plays the most
90 important role in the fate of atmospheric NO_x, HONO, HCHO, or H₂O₂ emitted by the snow pack.
Key parameters are surface turbulent fluxes and the height of the boundary layer, which is
determined by vertical turbulent diffusion. These parameters are used in companion papers to](#)

determine the contribution of turbulence to the concentration of key atmospheric species emitted from the surface, driving the oxidant budget in the [near-surface atmosphere](#) at Dome C. [MAR](#)
95 [turbulent vertical diffusion coefficients](#) are used by [Preunkert et al. \(2014\)](#) and the uncertainty of
the later on [HCHO mixing ratios](#) is discussed. [Legrand et al. \(2014\)](#) also use the same [MAR outputs](#)
to force their 1-D box model to simulate [HONO mixing ratios](#). [Kukui et al. \(2014\)](#) performed similar
calculations using the same [MAR output](#). [Frey et al. \(2014\)](#) use [MAR boundary layer heights](#) to
determine when they may apply the [Monin–Obukhov similarity theory](#) for calculating the
100 [turbulent fluxes of NOx in the surface boundary layer](#). Other parameters like cloud cover and wind
direction are considered [for chemical analyses](#). For example situations with an overcast sky were
not considered nor situations for which the wind direction is from Concordia station, since the air
is then contaminated by pollutants emitted by the station. [Sunny sky conditions were preferred](#)
[since the assumption of a similar downward shortwave \(DSW\) radiation from sunny day to sunny](#)
105 [day may be done](#). From a meteorological point of view these criteria also allow us to avoid most of
the situations for which clouds are underestimated by [MAR](#) leading to an erroneous behaviour of
the surface energy budget, and subsequently of atmospheric turbulence, as explained by [Legrand](#)
[et al. \(2014\)](#). Fortunately such a behaviour of [MAR](#) allows us to analyze the best part of the
simulation which corresponds to the same days for which the analysis of chemical species is the
110 [easiest](#).

The remaining of the paper is divided in 4 parts. The experimental set-up and the main characteristics of the [MAR](#) model are described in sections 2 and 3. The fourth section is dedicated to the evaluation of the model, looking in particular at the impact of the simulated radiative transfer on the surface atmospheric energy budget and atmospheric turbulence.

115

2. Meteorological observations

2.1. ISAC (*Istituto di Scienze dell' Atmosfera e del Clima*)

120 One-year in situ turbulence and radiation measurements, as well as sodar observations, were carried out at the Concordia station from December 2011 up to December 2012 as part of the ABLCLIMAT project (Argentini et al., 2013).

The SL-sodar (Surface Layer sodar, Argentini et al., 2011) is an improved version of the sodar described by Argentini and Pietroni (2010), with the possibility of zooming into the atmospheric
125 surface-layer thermal turbulent structure. With the SL-Sodar, the PBL height h is estimated following Casasanta et al. (2014). During convective conditions h was determined as the height above the zone of weak backscattered intensity of the acoustic waves emitted by the sodar. Under stable conditions, h was retrieved either from the minimum of the first derivative of the backscattered signal, or from its maximum curvature.

130 Measurements of turbulence were made with a Metek USA-1, a three-axes sonic thermo-anemometer (sampling frequency of 10 Hz) installed on a 3.5 m mast. The heat and momentum fluxes are estimated using the eddy covariance method. [The longwave and shortwave radiation components \(up and down\) were measured with a Kipp & Zonen CNR1 radiation sensor. This instrument combined two CM3 pyranometers for downward and upward broadband shortwave
135 radiation flux \(spectral range 305–2800 nm\) and two CG3 pyrgeometers for downward and upward broadband longwave radiation flux \(spectral range 5– 50 \$\mu\$ m\). Pyrgeometers and pyranometers were installed 1.5 m above the snow surface.](#)

2.2. LGGE (Laboratoire de Glaciologie et de Géophysique de l'Environnement)

140 Meteorological measurements were made on a 45-m tower at Dome C since 2008 (Genthon et al. 2010). Wind, temperature and moisture are monitored at six levels from the near surface (3.5 m) to near the top of the tower (42.1 m). The instruments occasionally fail due to the extreme weather conditions at Dome C (extreme low temperatures, frost deposition), however the data record is almost continuous since 2009 and the instruments work generally quite well in summer
145 (Genthon et al. 2013). Genthon et al. (2011) have demonstrated that a bias to warmer temperatures affects measurements in Antarctica in cases of weak winds if conventional passively (wind) ventilated radiation shields are used to protect solid state thermometers (e.g. the ubiquitously used platinum thermistors) from solar radiation. To overcome this problem the temperature measurements on the tower at Dome C are made in aspirated shields. Further details
150 of the profiling set up, instrumentation and results obtained so far can be found in Genthon et al. (2010, 2013).

2.3. BAS (British Antarctic Survey)

Measurements of turbulence are made with a Metek USA-1, a three-axes sonic thermo-
155 anemometer (sampling frequency of 25 Hz) mounted on a mast 4 m above the snow surface. The mast was set up in the clean-air sector at about 1.2 km distance from the 45-m meteorology tower (map in Frey et al., 2013), at the site where the chemical trace gas species were measured during the OPALE campaign. Atmospheric boundary layer parameters such as friction velocity u_* and
Monin-Obukhov Length were computed from the three-dimensional wind components (u, v, w)
160 and temperature (Frey et al., 2014, this issue). Processing in 10-min blocks included temperature

cross-wind correction and a double coordinate rotation to force mean w to zero (Kaimal and Finnigan, 1994; Van Dijk et al., 2006).

3. Description of MAR

165 An overview of the regional climate model MAR is given here, focused on the description of the turbulence scheme. A more complete description can be found in Gallée and Schayes (1994), Gallée (1995) and Gallée et al. (2013).

MAR atmospheric dynamics are based on the hydrostatic approximation of the primitive equations. This approximation is correct when the vertical extent of the circulation (here the drainage flow) remains much smaller than the size of the grid (here 20 km). Nevertheless, it should be noted that non-hydrostatic processes may be responsible for a weak deceleration of the katabatic flow (Cassano and Parish, 2000). The vertical coordinate is the normalized pressure, with the model top situated at the 1 Pa pressure level. Parameterization of turbulence in the surface boundary layer is based on the Monin-Obukhov [similarity](#) theory (MOST) and is completed by taking into account the stabilization effect by the blowing snow flux, as in Gallée et al. (2001) (see also Wamser and Lykossov, 1995). Turbulence above the surface boundary layer is parameterized using the local $E - \epsilon$ model, consisting in two prognostic equations for turbulent kinetic energy and its dissipation. The prognostic equation of dissipation allows to relate the mixing length to local sources of turbulence and not only to the surface. The $E - \epsilon$ model used here has been adapted to [neutral and](#) stable conditions by Duynkerke (1988) and revised by Bintanja (2000), who included a parameterization of the turbulent transport of snow particles that is consistent with classical parameterizations of their sedimentation velocity. The influence of changes in the water phase on the turbulence is included following Duynkerke and Driedonks (1987). The relationship between

170
175
180

the turbulent diffusion coefficient for momentum and scalars (Prandtl number) is dependant on
185 the Richardson number, according to Sukoriansky et al. (2005).

Prognostic equations are used to describe five water related parameters (Gallée, 1995): specific
humidity, cloud droplets and ice crystals, raindrops and snow particles. A sixth equation has been
added describing the number of ice crystals, and the influence of hydrometeors on air specific
mass is included in the model (Gallée et al. (2001). This allows us to account for the influence of
190 the weight of eroded particles on atmospheric flow dynamics by representing the pressure
gradient force as a function of air density rather than of potential temperature only.

The radiative transfer through the atmosphere is parameterized following Morcrette (2002) and is
the same as the one used in ERA-40 re-analyses. As blowing snow particles are small (Walden et
al., 2003), they may have an impact on the radiative transfer. Influence of snow particles on
195 atmospheric optical depth is also included in the MAR model (Gallée and Gorodetskaya, 2010).

Surface processes are modelled using the “soil-ice-snow-vegetation-atmosphere transfer” scheme
(SISVAT, De Ridder and Gallée, 1998, Gallée et al., 2001, Lefebvre et al., 2005, Fettweis et al., 2005).

The influence of snow erosion / deposition on surface roughness (z_0) is taken into account by
allowing the aerodynamic roughness length to increase linearly as a function of the wind speed at

200 10 m above the ground level (a.g.l.) (V_{10}), when $V_{10} > 6 \text{ m s}^{-1}$. The time scale for sastrugi

formation is assumed to be half a day, as suggested by Andreas (1995), and the asymptotic value of

the surface roughness length z_0 may increase linearly as a function of the wind speed $V(z_{0,lim} =$

1.5 mm for $V = 10 \text{ m s}^{-1}$; note that the friction velocity corresponding to $V = 10 \text{ m s}^{-1}$ is generally

slightly greater than 0.5 m s^{-1}). z_0 is allowed to decrease when precipitation occurs without wind
erosion of the snow. Indeed the newly deposited snow progressively buries the sastrugi. Andreas
et al. (2005) found values of z_0 ranging between approximately 10^{-4} and 100 mm, for friction
velocities no greater than 0.6 m s^{-1} . King and Anderson (1994) observed at Halley for compacted,
sintered firn with some sastrugi, i.e. for similar snow properties as encountered at Dome C, a z_0
value of $(5.6 \pm 0.6) \times 10^{-5}$ m. The scatter of z_0 is very high and is explained by the high dependency
of z_0 on sastrugi history. Our parameterization includes that effect in a simple way, and is
calibrated to obtain the best simulation of the wind speed. [Note that the snow surface albedo depends on the snow properties \(dendricity, sphericity and size of the snow particles\) and solar zenithal distance, but not on sastrugi nor sastrugi orientation.](#)

215 4. Evaluation of MAR

We here used the 3-D version of MAR in order to take into account the influence of drainage winds on mass divergence at Dome C and consequently on subsidence and thinning of the boundary layer at the dome. In addition this allows also to account for a possible influence of the inversion wind circulation over the Dome C area, as suggested by Pietroni et al. (2014). The MAR domain is
220 represented in Fig. 1. The horizontal grid size is 20 km and the vertical discretization in the lower

troposphere is 2 m, with 60 levels. The vertical resolution decreases with altitude above 32 m a.g.l., reaching 50 m at 300 m a.g.l. and 400 m at 3000 m a.g.l. In parallel MAR was also run with a vertical grid spacing of 1 m in the lower levels, without any significant change [in the results](#). Taking advantage of the higher vertical resolution near the surface the output of this latter model run was used to discuss the behaviour (in particular the diurnal cycles) of different atmospheric components as e.g. HONO, ROH, NO_x, and HCHO, measured near the surface during the OPALE campaign (Legrand et al., 2014; Kukui et al., 2014; Frey et al., 2014; and Preunkert et al., 2014).

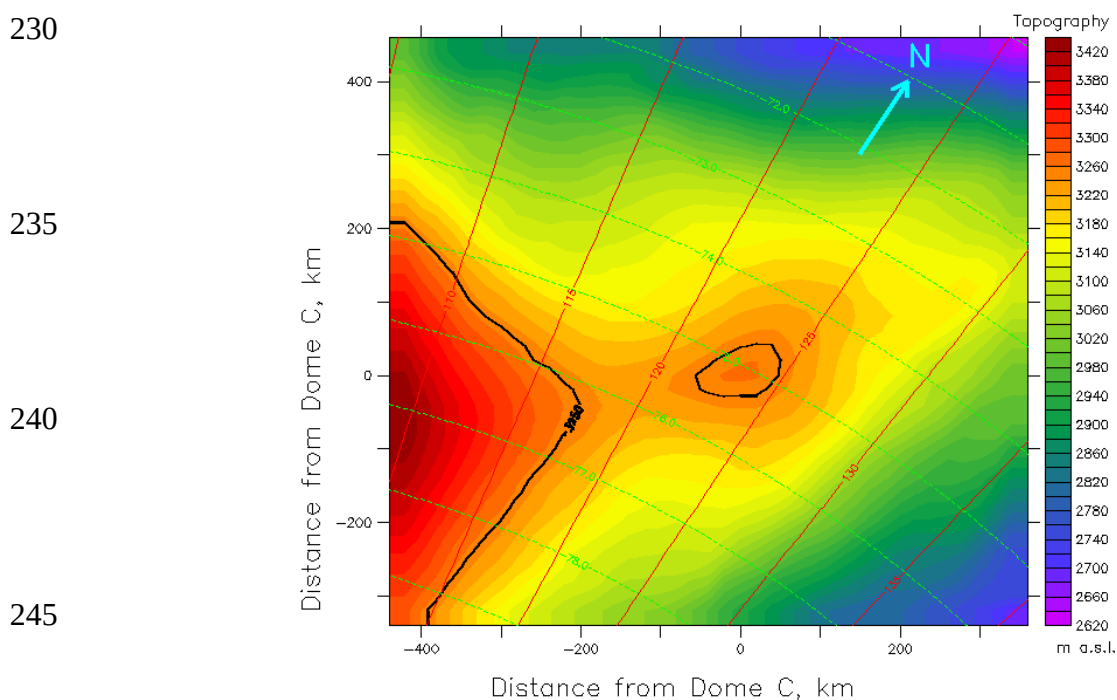


Fig. 1. The MAR integration domain and topography. The solid line refers to the 3250 m isocontour.

The MAR model is nested into the European re-analyses ERA-Interim (Dee et al., 2011). A relaxation zone of 5 grid points is prescribed at each lateral boundary (Marbaix et al., 2003) and model variables are nudged to the re-analysed variables in the upper 6 layers, i.e., above 13 km a.g.l. at Dome C. As the OPALE campaign took place from early December 2011 until mid January

2012, MAR was run over 3 months (from 1 November 2011 until 31 January 2012). The model variables are assumed to adapt to Dome C conditions during the first simulated month (i.e., November 2011). The snow pack is initialized with a density of 300 kg m^{-3} and the assumption of the presence of small grains, what results in a slightly decreased initial albedo (close to 0.79 at noon), compared to the value (0.80-0.81) estimated by Brun et al. (2011). Note that the albedo would have been more underestimated if sastrugi orientation had been taken into account (Wendler and Kelley, 1988). However no observation of sastrugi has been made during the OPALE campaign. Our analysis focuses on the period between 12 December 2011 and 14 January 2012, when most of the OPALE observations were made.

265 **4.1. Cloud cover and surface energy budget**

A problem already encountered when running the model over Adélie Land (East Antarctica) is an underestimation of the cloud cover (but not always) and the subsequent underestimation (overestimation) of the downward long-wave (shortwave) radiation. As a consequence, an underestimation (overestimation) of air temperatures near the surface during night-time (day-time) results (Gallée et al., 2013).

In the following we will investigate in how far this shortcoming occurs also in the MAR simulations at Dome C. We note first that MAR generally underestimates both the short-wave and long-wave downward radiations, with a bias of about 24.3 W m^{-2} and 20.8 W m^{-2} , respectively (Table 1). The influence of the former on the surface energy budget is nevertheless less important than that of the latter, because of the high value of the snow albedo.

MAR		ISAC	ISAC 3 m	Tower 3 m	BAS 4 m
SWD	Bias	-24.3 W m ⁻²			
SWA	Bias	3.4 W m ⁻²			
LWD	Bias	-20.8 W m ⁻²			
Temperature	Corr. Coef.		0.981	0.912	0.973
	Bias		-0.387 °C	-0.642 °C	-0.551 °C
	RMSE		2.408 °C	2.778 °C	2.735 °C
	E		0.958	0.751	0.933
Wind Speed	Corr. Coeff.		0.865	0.872	0.856
	Bias		-0.227 m/s	-0.105 m/s	0.440 m/s
	RMSE		1.057 m/s	0.949 m/s	1.089 m/s
	E		0.737	0.752	0.677

280 **Table 1.** Correlation coefficient, bias, RMSE (root mean square error) and efficiency statistical test
of the simulated short-wave downward radiation (SWD), the short-wave absorbed radiation by the
surface (SWA), the long-wave downward radiation (LWD), the temperature and the wind speed
when compared to the observations made by **ISAC** (Istituto di Scienze dell' Atmosfera e del Clima) (3
rd and 4th column), by **LGGE** (Laboratoire de Glaciologie et de Géophysique de l'Environnement) (at
285 the tower, 5th column) and by **BAS** (British Antarctic Survey) (6th column). Data were averaged over
an interval of 30 minutes.

Let us now examine the downward long-wave radiation and the air temperature near the surface
(Fig. 2). Both observations and simulation exhibit rapid variations in the long-wave downward
290 radiation (LWD) (Fig. 2a). The correlation coefficient between the simulated LWD and cloud optical
thickness is 0.79 for a 10 minutes time interval between each value of these variables, suggesting
that cloud cover changes are responsible for most of these variations.

Fig. 2b compares the daily averaged bias (simulation minus observation) in the long-wave
downward radiations (LWD) and air temperatures near the surface at Dome C. The former is
295 generally underestimated, leading to the underestimation of the latter (see also Table 1). A
significant correlation may be seen between both biases, even when the temperature bias may be

positive while the long-wave downward radiation bias remains negative. But the latter bias is partially compensated by a slight positive bias in the absorbed solar radiation (Table 1), probably because of an underestimation of MAR snow surface albedo.

300 In contrast, the bias in the absorbed solar radiation may become negative, for example on 10 and 11 January 2012, when the bias in the long-wave downward radiation is almost zero and significant snowfall is simulated. The positive temperature bias on 31 December 2011 is probably due to an overestimation of the long-wave downward radiation by MAR.

Thus, as already observed along the Adélie Land Coast (see Gallée et al., 2013), MAR
305 underestimates cloud cover at Dome C, but not always. This underestimation is responsible for an underestimation of the downward long-wave radiation. As long-wave downward radiation plays a key role in the surface energy budget and the subsequent behaviour of turbulence near the surface, this point will be considered in the remaining of the paper. Concerning the application of MAR for the interpretation of the atmospheric chemistry measured during OPALE, the
310 underestimation of the cloud cover is generally not critical since situations with an overcast sky were not considered in these model applications.

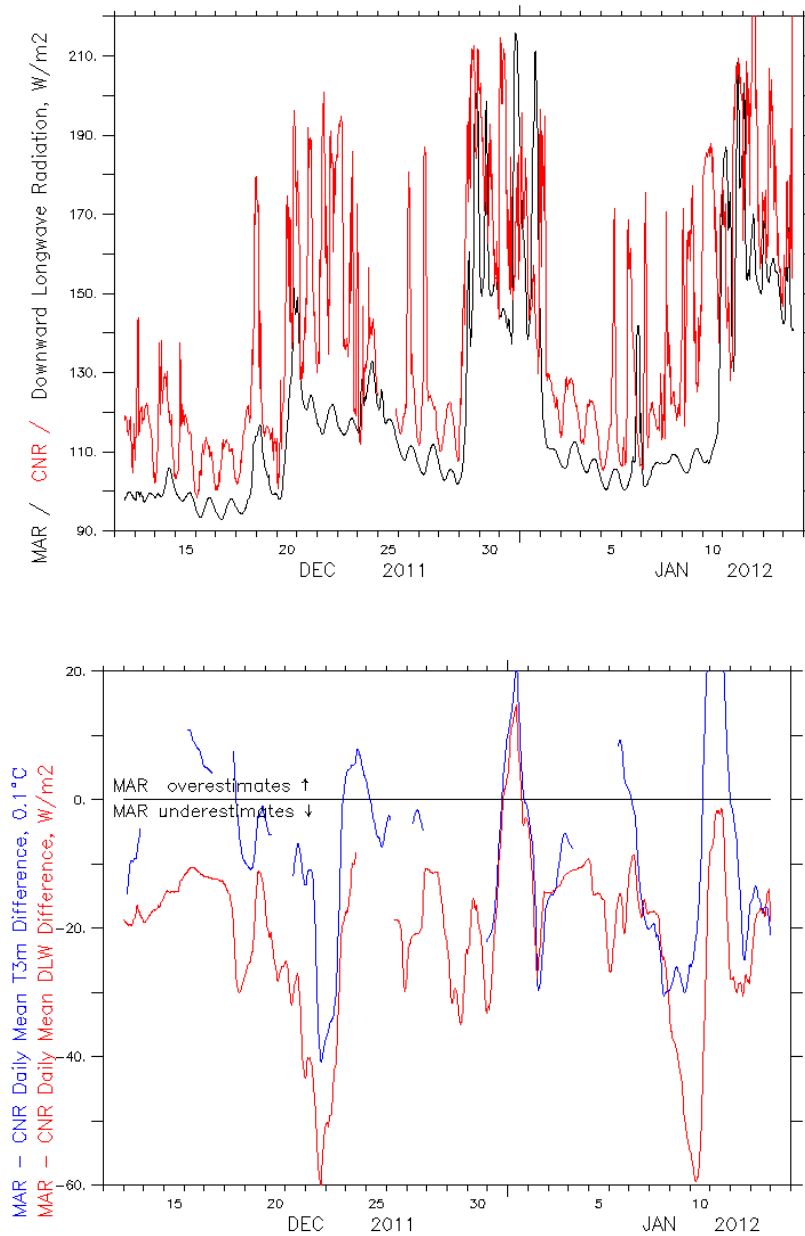


Fig. 2. Top : Long-wave Downward radiation (LWD, W/m^2) : simulation (dark line) and observation (red line). Data were averaged over an interval of 30 minutes. Bottom : comparison between the daily averaged LWD bias (red line) and air temperature bias (blue line, units : $0.1^\circ C$). Observations are those of the ISAC. MAR temperatures are averaged between 2 m and 4 m a.g.l. Gaps correspond to the absence of observations.

4.2. Wind and Temperature near the surface

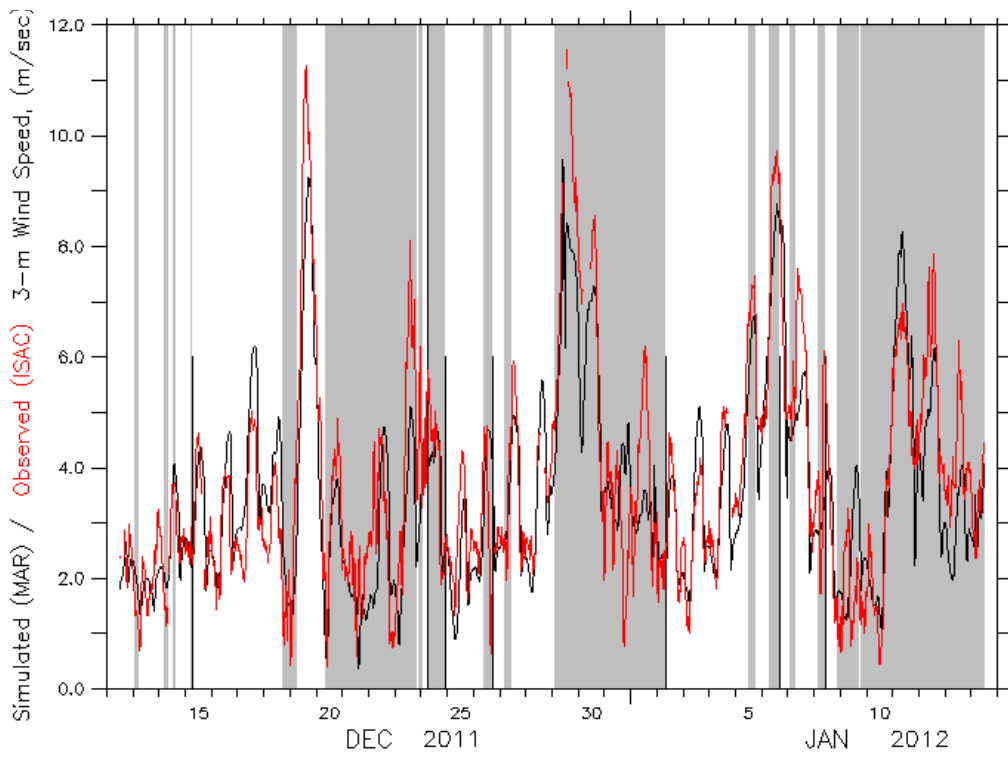
The performances of the simulated temperature and wind speed are summarized in Table 1 by the
325 correlation between simulation and observation, the bias (simulation minus observation), the root
mean square error (RMSE) and the efficiency statistical test (E) proposed by Nash and Sutcliffe
(1970):

$$E = 1 - \frac{RMSE^2}{s^2} \quad (2)$$

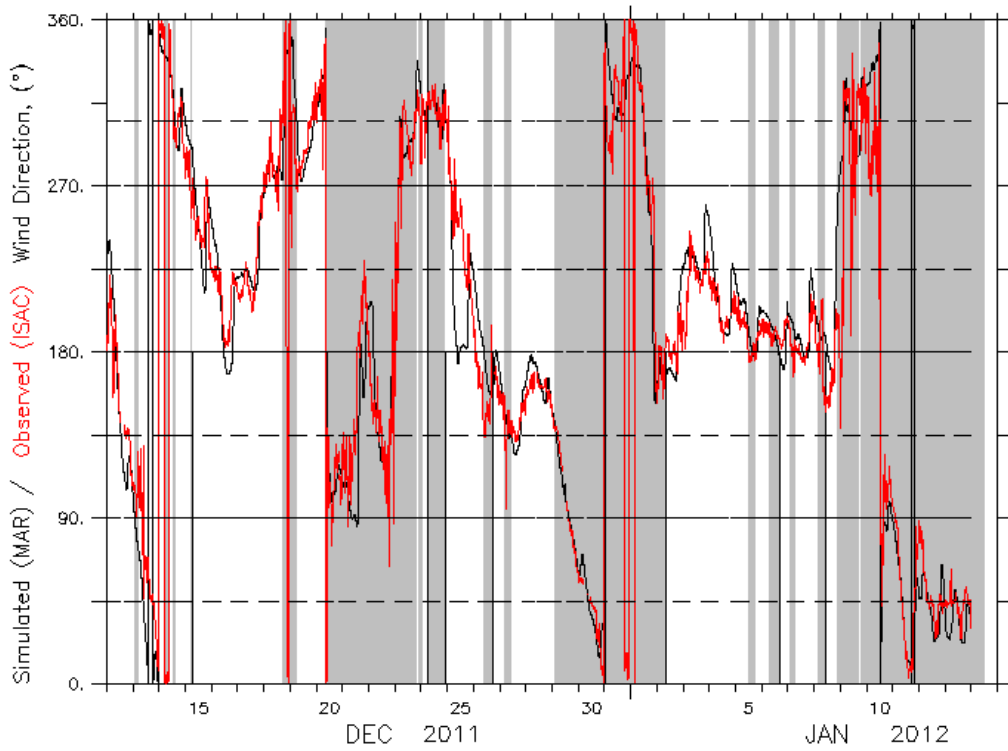
where s and $RMSE$ are respectively the standard deviation of the observations and the root-mean-
330 square error of the simulated variable. Note that $RMSE = 0$ implies $E = 1$. An efficiency index
greater than 0 also means that comparing the simulated variable with the corresponding
observation provides a lower $RMSE$ than that obtained when comparing it with its time average. A
negative efficiency index means that the $RMSE$ is higher than the standard deviation of the
observations. Finally, this then suggests that a detailed model would not improve the results when
335 compared to a simpler model providing an estimation of the variable averaged over the time
period concerned.

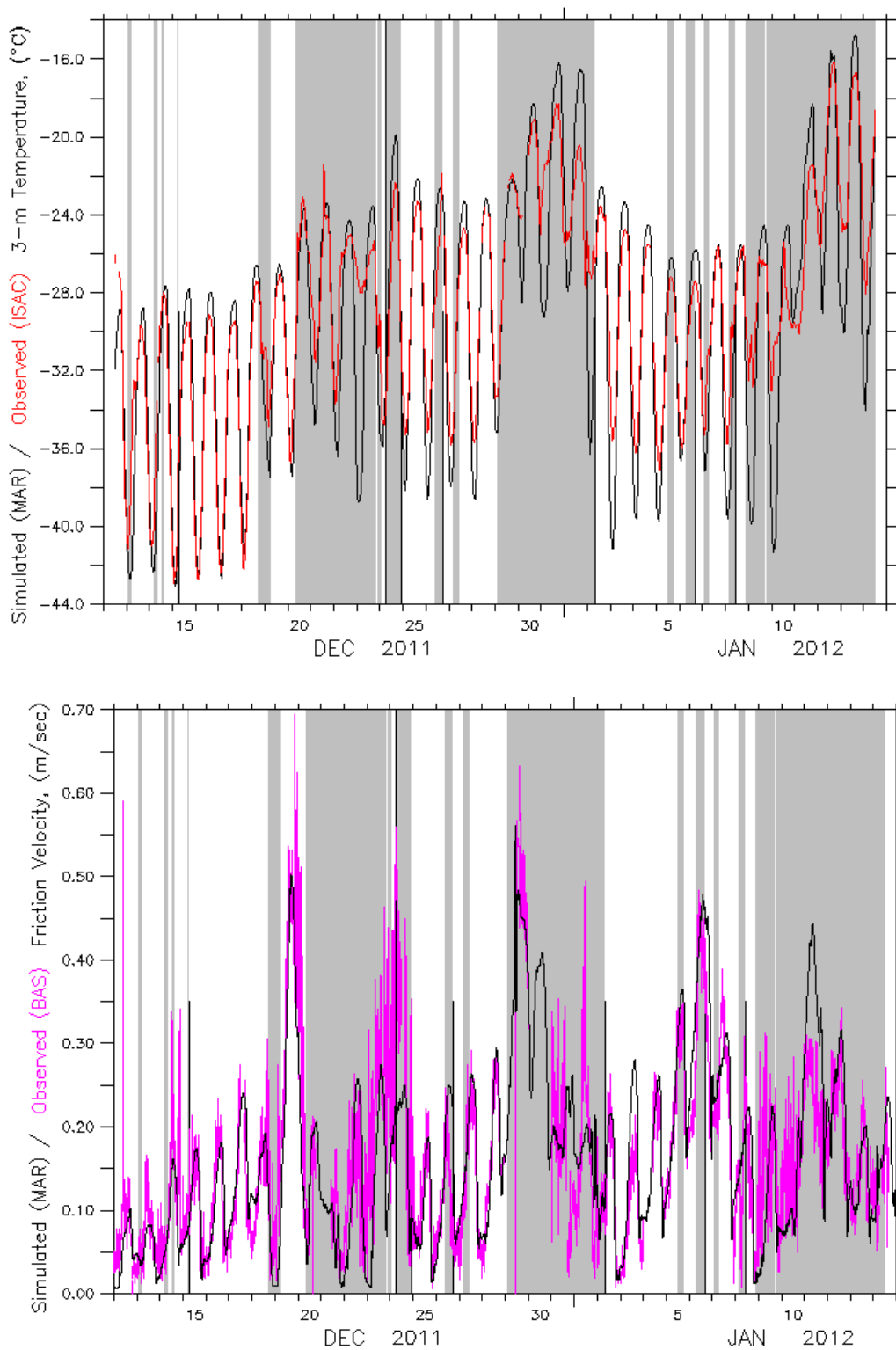
It is found that the efficiency statistical test for temperature and wind speed is not lower than
0.677 for all comparisons (Table 1) giving us confidence into the respective time averages as well as
into the fluctuations of these simulated variables.

340



345





350

Fig. 3. Simulation (dark line) of wind speed (top left), wind direction (top right), and air temperature (bottom left) at Dome C, 3 m a.s.l., compared with ISAC observations. Bottom right: simulation of friction velocity (dark line) compared with BAS observations (magenta line). Data were averaged over an interval of 30 minutes. Shaded area indicate periods with DLW > 130

-2

355

Wm

For a more detailed examination of wind speed and temperature, the comparison between simulated and observed wind speeds at 3 m above the surface is shown in figure 3a. The agreement is good, as also quantified by the efficiency (0.737, Table 1). As it can be seen in Fig. 3b the agreement between the simulated and observed wind direction is also excellent. This behaviour indicates that the model is able to capture the atmospheric circulation at Dome C at the synoptic scale and is able to simulate the local circulation. Both, observation and simulation reveal two preferential wind directions, one from the plateau (southerly winds) and the other from the ocean (northerly winds). A well-marked diurnal cycle is generally found in the wind speed but does not exist in the wind direction. Wind speed peaks during the afternoon, when turbulent fluxes in the well mixed layer are able to transport momentum downwards more efficiently. Wind speed is also generally stronger and may be larger than 6 m s^{-1} in case of wind blowing from the North, except on 5 - 7 January 2012, when wind was blowing from the South. Note that the simulation of a blowing snow event on 29 December is responsible for an increase of the simulated roughness length from an almost constant in time value of 0.05 mm to an almost constant in time value of 2 mm. No significant change in the agreement between simulation and observations of the wind speed or of the friction velocity after this increase may be deduced from a look to Fig. 3. Consequently it is difficult to determine if the parameterization of the roughness length at Dome C is important for the simulation.

The simulated air temperature is also in good agreement with observations (Fig. 3c), although the simulated diurnal cycle is generally more pronounced than the observed one, especially for night-time (not shown for tower and BAS observations). The largest differences are found when simulations are compared with the observations made at the tower. Note that, tower temperature measurements are performed in aspirated shields which have been demonstrated to avoid large warm biases with the most often used passively ventilated shields in cases of weak winds (Genthon

380 et al. 2011). Since these are the only temperature measurements carried out in aspirated shields at Dome C, they are (except of sonic measurements) the only ones which are unaffected by radiations biases.

Finally the good behaviour of the simulated friction velocity (Fig. 3d) suggests that MAR simulates surface meteorological variables without compensating errors. From the previous analysis we have 385 some confidence on the behaviour of the model in the surface boundary layer at Dome C during the OPALE observation period, but some discrepancies with the observations are found, even for sunny days.

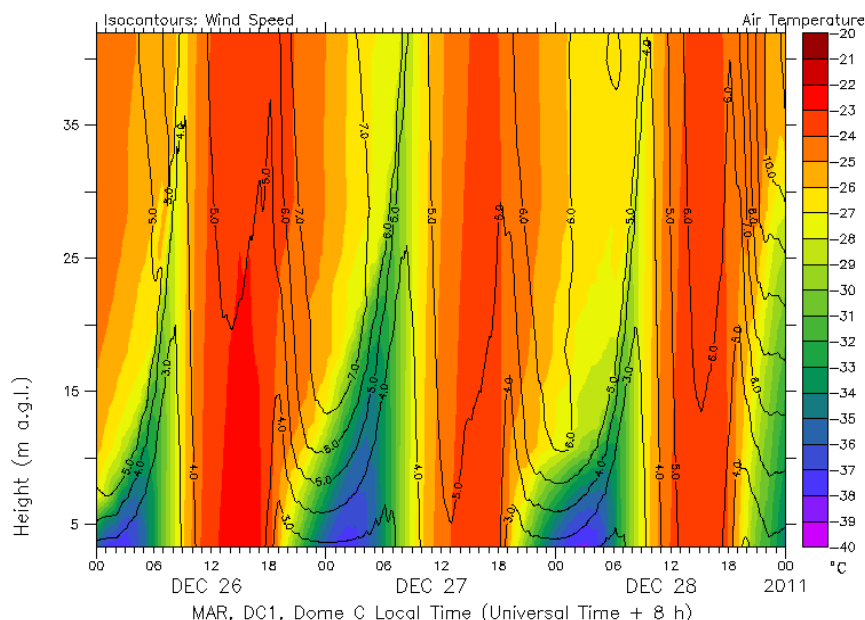
4.3. Period between 26 and 28 December 2011

390 In the following we will focus on the period between 26 and 28 December 2011, which is also included in the studies of Legrand et al. (2014), Kukui et al. (2014), Preunkert et al. (2014), and Frey et al. (2014). Moreover this is the longest period for which we have estimations of the boundary layer height from sodar measurements. This period is characterized by winds coming from the high East Antarctic plateau and by an absence of clouds except between 9 h LT and 15 h LT on 26 395 December and between 4 h LT and 11 h LT on 27 December, when the downward long-wave flux (LWD) is relatively large in the observations. Unfortunately MAR underestimates LWD at those times (see section 4.1 and Fig. 2a).

In Fig. 4a we report the behaviour of the simulated temperature and wind speed at the tower, between 3.5 and 42.1 m a.g.l. The simulation exhibits a marked diurnal cycle, with a strong 400 temperature inversion during night-time and a well mixed layer during day-time. During night-time a close link exists between the vertical temperature gradient and the vertical wind speed gradient. The vertical wind speed gradient is the highest where temperature increase with height is the strongest and associated vertical stability is the largest. Such a behaviour is often referred to as a

decoupling between the cold air near the surface and the warmer air above. This decoupling is also
 405 found in a change of the wind direction just above the turbulent layer. Convective mixing during
 day-time precludes this behaviour, and the vertical gradients of both temperature and wind speed
 are much smaller. Night-time decoupling and day-time mixing are also found in the observations,
 but with some differences due to the presence of clouds that the model was not able to simulate.

It is seen in Fig. 4b that the model simulates a warm bias on 26 December 2011 until 18 h LT,
 410 except below 10 m a.g.l. until 6 h LT. Probably the absence of simulated clouds is responsible for an
 overestimation of the surface absorbed solar radiation and the subsequent heating of the surface.
 The heat excess is then transferred to the atmosphere through turbulent mixing. Note that the
 marked overestimation of the simulated absorbed solar radiation and air temperature are not
 repeated on 27 and 28 December 2011 in spite of the presence of clouds on December 27 in the
 415 morning. Nevertheless temperature maxima are overestimated by roughly 1 to 1.5°C, both at the
 surface (not shown) and above.



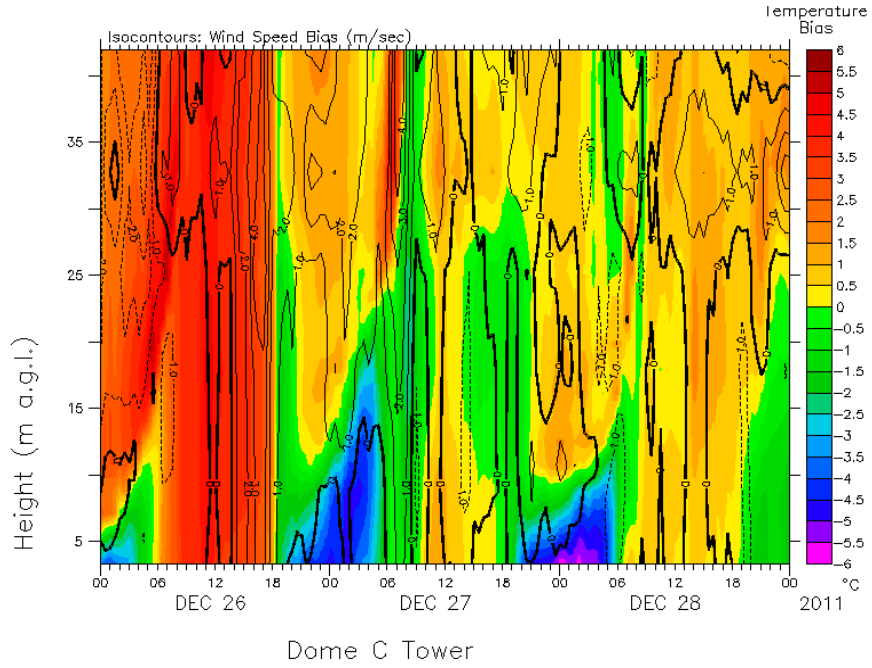
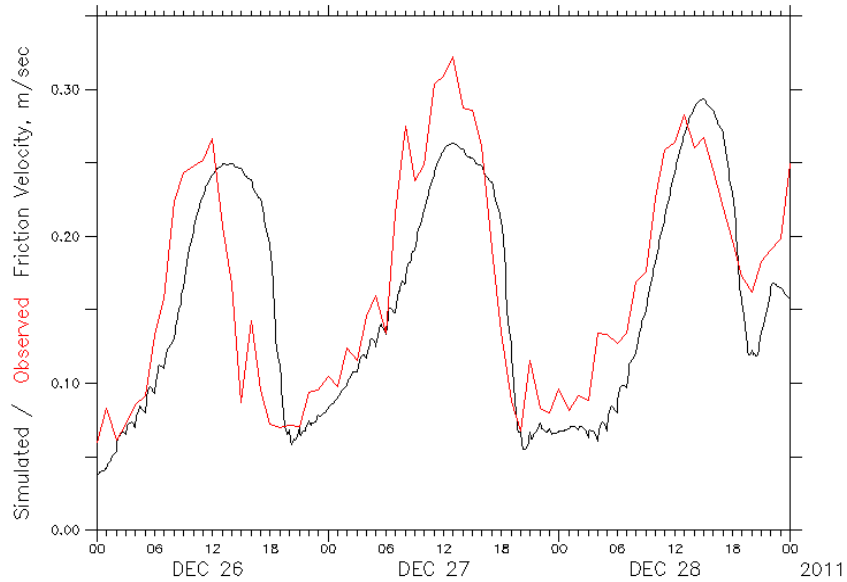


Fig. 4. Temperature (color) and wind speed (isocontours) at the Dome C tower, as a function of Local Time LT (Universal Time UT + 8 h) and height above the surface. (a) refers to MAR simulation, (b) to simulation minus observation.



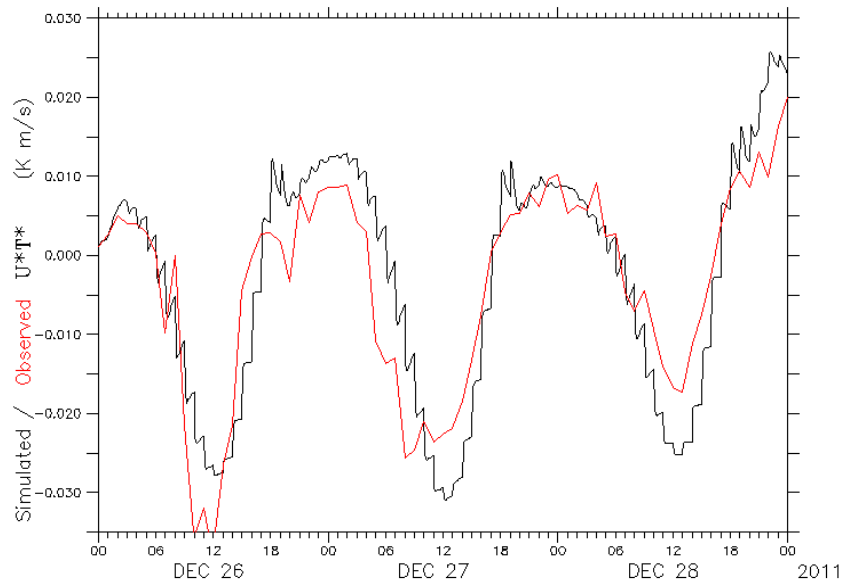


Fig. 5. Surface turbulent fluxes at the Dome C tower, as a function of Local Time LT (Universal Time UT + 8 h). The panel a refers to the friction Velocity, the panel b to the sensible Heat Flux u^*T^* . The dark line is the MAR simulation, the red line the ISAC observations.

430

435 Air temperatures on 27 and 28 December in the morning are significantly underestimated in the MAR simulations, especially on 28 December. [The underestimation starts previous day around 18 LT.](#) An underestimation of about 10 W m^{-2} or more is also found in the downward long-wave radiation (LWD), even in the absence of clouds (Fig. 2a). Simulated and observed turbulent fluxes are compared in Fig. 5. The simulated friction velocity is slightly underestimated by the MAR model during night-time, especially on 28 December, while the simulated downward turbulent heat flux is comparable to the observations or slightly overestimated. Possibly the simulated surface turbulent heat flux would have been larger if the friction velocity had not been underestimated by the model at that time. Thus Monin-Obukhov Similarity Theory is not a good candidate for explaining the underestimation of temperature near the surface. More precisely [looking at the experiment with 1](#)

440

445 m resolution it is found that the weakening of the turbulent fluxes from 1 to 2 m amounts to slightly more than 20%, a value that is larger than the usual departure from constancy generally accepted (10%). More generally temperature and wind speed at 2 m in the simulations with 1 m and 2 m resolution near the surface have been compared. It has been found that when clear sky is observed they are not sensitive (differences no larger than 1.5°C to 2°C or 1 m/sec) to the vertical
450 resolution even when in the simulation with 1 m resolution the turbulent fluxes between 1 m and 2 m depart from the constancy by 30%. In contrast a slight overestimation of the air temperature above 10 – 15 m a.g.l. (Fig. 4b) could also result from an insufficient turbulent mixing by the $E - \epsilon$ model during night-time, explaining also partly the underestimation of the air temperature near the surface. Finally it could be argued that an initial underestimation of the air temperature near
455 the surface may be responsible for an increased vertical stability above the surface boundary layer, reinforcing the decoupling between the lower troposphere and the atmosphere above, and being responsible for a possible underestimation of the boundary layer height. A possible leading role of an underestimation of LWD must be firmly established.

From Fig. 5 it is also found that MAR underestimates the upward turbulent heat flux during day-
460 time, when observed clouds were not simulated (on 26 December around noon and on 27 December in the morning) while it overestimates it when clouds are not present nor in the observation nor in the simulation (on 27 and 28 December during day-time). No definite explanation was found about the underestimation but the overestimation may be related to a too large heating of the surface and an overestimation of the air temperature by the model (see Fig.
465 4b), suggesting that the overestimation of air temperature at that time is driven by the surface.

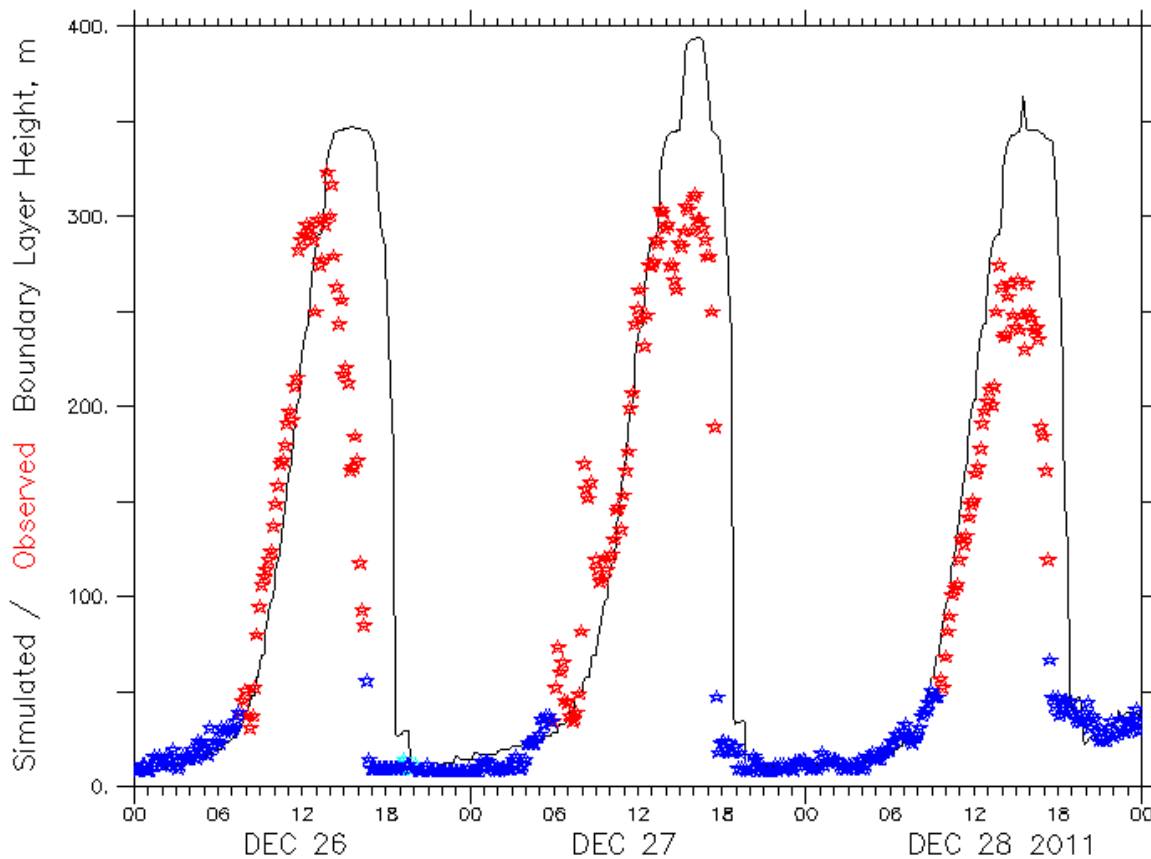


Fig. 6. The boundary layer height at Dome C as a function of Local Time LT (Universal Time UT + 8 h). Red (blue) stars: SODAR observations during convective (stable) situations (Argentini et al., 2013). Dark line : MAR mixed layer depth, computed as the level where the turbulent kinetic energy amounts to 5 % of the turbulent kinetic energy in the lowest layer of the model.

470

Biases in the simulated wind speed could be sometimes linked to biases in the simulated air temperature but not always. An example of such a link in Fig. 4b is a positive wind speed bias simulated between 15 h and 18 h LT on 26 December 2011. It could be associated with the positive bias in the downward short-wave radiation. At that time the overestimated turbulent mixing could

475

lead to an overestimated height of the turbulent layer and an overestimated downward transfer of momentum. Indeed simulated wind speeds are larger than observations at the upper levels of the tower at that time (Fig. 4a) and the model overestimates the height of the well-mixed layer (Fig. 6).

The bias in the wind speed decreases after 18 h LT especially below 25 m a.g.l. This is due to an increasing stability near the surface and the subsequent decoupling between the layer of air near

480

the surface and the layer above. Wind speeds are still overestimated above up to the highest level of the tower, possibly because of an overestimated vertical extent of the residual mixed layer at

that time.

Observations suggest the onset of a nocturnal jet after 18 h LT, with a maximum of 7 m s^{-1} around 20 m a.g.l. around 22 h LT. MAR also simulates a nocturnal jet at that time but around 140 m a.g.l.,
485 and with a slightly stronger wind speed (8 m s^{-1}) (not shown). This occurrence is consistent with a higher extent of the residual layer and may be the consequence of the sudden shut down of the turbulent mixing at 18 h LT at 140 m a.g.l. in the model (not shown), while the pressure gradient force (PGF) still contributes to an increase of the wind speed after that time. Such an evolution is typical for a convective mixed layer at the end of day-time, and is also observed at lower latitudes.
490 The contribution of PGF to the acceleration of the wind starts to decrease after 20h30 LT. Since nocturnal low level jets arrived frequently during OPALE the analysis of this process deserves some attention. Therefore, this topic will be addressed in a companion note by analysing a case study which is well simulated by the model (Gallée et al., 2014, this issue).

A small positive temperature bias seems also to occur on 6 h LT on 27 December 2011 above 25 m
495 a.g.l. Its behaviour is similar to that of 26 December and it occurs also in conjunction with an underestimation of the cloud cover by the model and an earlier deepening of the well-mixed layer.

Finally the sodar reveals an earlier peak and fall-off in boundary layer depth on 26 December than does the model (Fig. 6). This is due to clouds which are responsible for a strong decrease of SWD, while clouds are not simulated.

500 **5. Discussion and conclusion**

The MAR model has been set up over a domain covering Dome C during the OPALE campaign. The size of the domain is much smaller than the internal radius of deformation. As a consequence the model solution is constrained in the free atmosphere by the one of the European re-analyses ERA-Interim but, as already pointed out by Lefebvre et al. (2005), it allows to develop its own solution in

505 the boundary layer. The simulation is characterized by a positive efficiency of wind and temperature over Dome C, given us confidence in its behaviour. In certain situations, MAR underestimates the downward long-wave radiation. When this problem occurs it is often linked to an underestimation of the cloud cover, and is one of the reasons , which leads to an overestimation of the simulated amplitude of the diurnal cycle of air temperatures. An other
510 possible cause of this overestimation is the underestimation of heat transfer in the snow pack and an amplification of the subsequent decoupling between the atmosphere and the surface initiated by the underestimated LWD and heat conduction. Indeed surface turbulent fluxes are well simulated, but discrepancies with the observations are found when the simulated downward long-wave flux is underestimated. *Note that, since this underestimation of the LWD will induce also an
515 error in the modeled temperatures measured temperatures, which were available through all the OPALE campaign were used when interpreting the chemistry data (e.g. Preunkert et al., 2014).* On the other hand the simulated wind speed in the surface boundary layer is in good agreement with the observations. It may consequently be argued that the turbulence schemes used in MAR (Monin-Obukhov similarity theory and $E - \epsilon$ model) are valid for the OPALE period. However, the
520 question whether this keeps true also under strong radiational cooling as encountered during winter at Dome C is still open.

Consequently model outputs and especially its turbulent characteristic are useful when interpreting the observations made in case of observed clear sky during OPALE. Indeed clear sky conditions, i.e. situations for which the model simulation is in excellent agreement with available
525 observations, are more adequate when discussing measurements of species involved in photochemical processes. In particular the good behaviour of the simulated surface turbulent fluxes allows us to use the associated turbulent eddy diffusivity coefficient to evaluate the impact of turbulent transport on NO_x , HONO and HCHO emitted from snow. In addition the simulated

boundary layer height indicates over which thickness of the atmosphere these chemical species
530 are diluted. In brief, the use of such a model will allow us to optimize the experimental set- up for
future campaign aiming to characterize the low troposphere chemistry at Dome C.

Acknowledgments

The OPALE project was funded by the ANR (Agence National de Recherche) contract ANR-09-BLAN-
0226. Most of the computations presented in this paper were performed using the Froggy platform
535 of the CIMENT infrastructure (<https://ciment.ujf-grenoble.fr>), which is supported by the Rhône-Alpes
region (GRANT CPER07_13 CIRA), the OSUG@2020 labex (reference ANR10 LABX56) and the
Equip@Meso project (reference ANR-10-EQPX-29-01) of the programme Investissements d'Avenir
supervised by the Agence Nationale pour la Recherche. This work was also granted access to the
540 HPC resources of [TGCC/CINES/IDRIS] under the allocation 2014 - 1523 made by GENCI. IPEV-
CALVA, IPEV-CESOA, INSU-LEFE-CLAPA and OSUG GLACIOCLIM-CENACLAM projects are
acknowledged for their support. ABLCLIMAT research was supported by the Italian National
Research Programme (PNRA) in the frame of French-Italian projects for Dome C.

545

References

- Andreas, E.L. : Physically based model of the form drag associated with sastrugi. US Army Cold Regions
Research and Engineering Laboratory, Hanover, NH, CRREL Report No CR 95-16, 12pp, 1995.
- 550 Argentini, S. and Pietroni, I. : An Integrated Observing System for Boundary Layer Monitoring at Concordia
Station, Antarctica, in Integrated Ground-Based Observing Systems D. Cimini, F. Marzano and G. Visconti
(Editors), Springer-Verlag, Berlin Heidelberg, 199-208, 2010.
- Argentini, S., Pietroni, I., Mastrantonio, G., Petenko, I., and Viola, A. : Use of a high-resolution sodar to study
surface-layer turbulence at night. Bound-Lay Meteorol, 143, 177-188, 2011.
- 555 Argentini, S., Petenko, I., Viola, A., Mastrantonio, G., Pietroni, I., Casasanta, G., Aristidi, E., Genthon, C. : The
surface layer observed by a high-resolution sodar at DOME C, Antarctica. Ann Geophys-Italy, 56, 5,
10.4401/ag-6347, 2013.
- Bintanja, R. : Snowdrift suspension and atmospheric turbulence. Part I: Theoretical background and model
description. Bound-Lay Meteorol 95, 343 – 368, 2000.
- 560 Brun, E., Six, D., Picard, G., Vionnet, V., Arnaud, L., Bazile, E., Boone, A., Bouchard, A., Genthon, C., Guidard,
V., Le Moigne, P., Rabier, F., Seity, Y. : Snow/atmosphere coupled simulation at Dome C, Antarctica. J Glaciol,
52(204), 721 – 736, 2011.
- Casasanta G., Pietroni, I., Petenko, I., Argentini, S. : Observed and Modelled Convective Mixing-Layer Height
at Dome C, Antarctica. Bound-Lay Meteorol, 151 (3), 597 – 608. DOI 10.1007/s10546-014-9907-5, 2014.
- 565 Cassano, J.J., and Parish, T.R.: An analysis of the nonhydrostatic dynamics in numerically simulated Antarctic
katabatic flows. J Atmos Sci 57, 891-898, 2000.

- Dee, D. P., Uppala, S. M., Simmons, A. J., Berrisford, P., Poli, P., Kobayashi, S., Andrae, U., Balmaseda, M. A., Balsamo, G., Bauer, P., Bechtold, P., Beljaars, A. C. M., van de Berg, L., Bidlot, J., Bormann, N., Delsol, C., Dragani, R., Fuentes, M., Geer, A. J., Haimberger, L., Healy, S. B., Hersbach, H., Hólm, E. V., Isaksen, I., Kållberg, P., Köhler, M., Matricardi, M., McNally, A. P., Monge-Sanz, B. M., Morcrette, J.-J., Park, B.-K., Peubey, C., de Rosnay, P., Tavolato, C., Thépaut, J.-N. and Vitart, F. : The ERA-Interim reanalysis: configuration and performance of the data assimilation system. *Q J R Meteorol Soc* 137, 553–597. doi: 10.1002/qj.828, 2011.
- 570 De Ridder, K., and Gallée, H. : Land Surface–Induced Regional Climate Change in Southern Israel. *J Appl Meteorol* 37, 1470 – 1485, doi: 10.1175/1520-0450, 1998.
- Dommergue, A., Barret, M., Courteaud, J., Cristofanelli, P., Ferrari, C. P., and Gallée, H. : Dynamic recycling of gaseous elemental mercury in the boundary layer of the Antarctic Plateau. *Atmos Chem Phys*, 12 (22), 11027-11036, 10.5194/acp-12-11027-2012, 2012.
- Duynkerke, P.G. and Driedonks, A.G.M. : A model for the turbulent structure of the stratocumulus-topped atmospheric boundary layer. *J Atmos Sci* 44, 43 – 64, 1987.
- 580 Duynkerke, P. G. : Application of the E – ϵ Turbulence Closure Model to the Neutral and Stable Atmospheric Boundary Layer. *J Atmos Sci* 45, 865–880, 1988.
- EPICA community members : Eight glacial cycles from an Antarctic ice core, *Nature*, 429, 623–628, 2004.
- 585 Fettweis, X., Gallée, H., Lefebvre, F., and Van Ypersele, J. : Greenland Surface Mass Balance simulated by a Regional Climate Model and Comparison with satellite derived data in 1990-1991. *Clim Dynam*, 24, 623–640. doi 10.1007/s00382-005-0010-y, 2005.
- 590 Frey, M. M., Brough, N., France, J. L., Anderson, P. S., Traulle, O., King, M. D., Jones, A. E., Wolff, E. W., and Savarino, J.: The diurnal variability of atmospheric nitrogen oxides (NO and NO₂) above the Antarctic Plateau driven by atmospheric stability and snow emissions, *Atmos. Chem. Phys.*, 13, 3045–3062, doi:10.5194/acp-13-3045-2013, 2013.
- 595 Frey, M. M., Roscoe, H. K., Kukui, S., Savarino, J., France, J. L., King, M. D., Legrand, M., and Preunkert, S.: Atmospheric nitrogen oxides (NO and NO₂) at Dome C, East Antarctica, during the OPALE campaign, *Atmos. Chem. Phys. Discuss.*, 14, 31281-31317, 2014.
- Gallée, H., and Schayes, G. : Development of a Three-Dimensional Meso- γ Primitive Equations Model, Katabatic Winds Simulation in the area of Terra Nova Bay, Antarctica. *Mon Weather Rev* 122, 671 – 685, 1994.
- 600 Gallée H. : Simulation of the mesocyclonic activity in the Ross Sea, Antarctica. *Mon Weather Rev* 123, 2051 – 2069, 1995.
- Gallée, H., Guyomarc'h, G., and Brun, E. : Impact of Snow Drift on the Antarctic Ice Sheet Surface Mass Balance. Possible Sensitivity to Snow Surface Properties. *Bound-Lay Meteorol* 99, 1 – 19, 2001.
- 605 Gallée, H., and Gorodetskaya, I. Validation of a limited area model over Dome C, Antarctic Plateau, during winter. *Clim Dynam* 23(1), 61 – 72, doi: 10.1007/s00382-008-0499-y, 2010.
- Gallée, H., Trouvilliez, A., Agosta, C., Genthon, C., Favier, V., and Naaim-Bouvet, F. : Transport of snow by the wind: a comparison between observations made in Adélie Land, Antarctica, and simulations made with the Regional Climate Model MAR. *Bound-Lay Meteorol*, 146(1), 133-147; 10.1007/s10546-012-9764-z, 2013.
- 610 Genthon, C., Town, M.S., Six, D., Favier, V., Argentini, S. and Pellegrini, A. : Meteorological atmospheric boundary layer measurements and ECMWF analyses during summer at Dome C, Antarctica. *J Geophys Res-Atmos*, 10.1029/2009JD012741, 115, (D05104), 2010.

- 615 Genthon, C., Six, D., Favier, V., Lazzara, M., and Keller, L. : Atmospheric temperature measurement biases on the Antarctic plateau, *J. Atm. Oceanic Technol.*, DOI 10.1175/JTECH-D-11-00095.1 28, No. 12, 1598-1605, 2011.
- Genthon, C., Six, D., Gallée, H., Grigioni, P., and Pellegrini, P. : Two years of atmospheric boundary layer observations on a 45-m tower at Dome C on the Antarctic plateau, *J Geophys Res-Atmos*, 118, 3218–3232, doi:10.1002/jgrd.50128, 2013.
- 620 Kaimal, J. C., and Finnigan, J. J.: *Atmospheric Boundary-Layer Flows: Their Structure and Measurement*, 289 pp., *Oxford University Press*, 1994.
- Kerbrat, M., Legrand, M., Preunkert, S., Gallée, H., and Kleffmann, J.: Nitrous Acid at Concordia on the East Antarctic Plateau and its transport to the coastal site of Dumont d'Urville, *J. Geophys. Res.*, 117, D08303, doi:10.1029/2011JD017149, 2012.
- 625 Kukui, A., Legrand, M., Preunkert, S., Frey, M. M., Loisil, R., Gil Roca, J., Jourdain, B., King, M. D., France, J. L., and Ancellet, G.: Measurements of OH and RO₂ radicals at Dome C, East Antarctica, *Atmos. Chem. Phys.*, 14, 12373-12392, doi:10.5194/acp-14-12373-2014, 2014.
- 630 King, J.C. and Anderson, P.S. : Heat and water vapour fluxes and scalar roughness lengths over an Antarctic ice shelf. *Bound-Lay Meteorol* 69, 101-121, 1994.
- King, J. C., Argentini, S., and Anderson, P. S.: *Contrasts between the summertime surface energy balance and boundary layer structure at Dome C and Halley stations, Antarctica*, *J Geophys Res-Atmos*, 111, doi 10.1029/2005JD006130, 2006.
- 635 Lascaux, F., Masciadri, E., and Hagelin, S.: *Mesoscale optical turbulence simulations above Dome C, Dome A and South Pole*. *Mon. Not. R. Astron. Soc.* 411, 693–704, doi:10.1111/j.1365-2966.2010.17709.x, 2011.
- Lefebvre, F., Fettweis, X., Gallée, H., Van Ypersele, J., Marbaix, P., Greuell, W., and Calanca, P. : *Evaluation of a high-resolution regional climate simulation over Greenland*. *Clim Dynam*, 25, 99–116, doi 10.1007/s00382-005-0005-8, 2005.
- 640 Legrand M., Preunkert, S., Jourdain, B., Gallée, H., Goutail, F., Weller R., and Savarino, J.: Year round record of sur- face ozone at coastal (Dumont d'Urville) and inland (Concordia) sites in East Antarctica, *J. Geophys. Res.*, 114, D20306, doi:10.1029/2008JD011667, 2009.
- 645 Legrand, M., Preunkert, S., Frey, M., Bartels-Rausch, T., Kukui, A., King, M.D., Savarino, J., Kerbrat, M., and Jourdain, B: Large mixing ratios of atmospheric nitrous acid (HONO) at Concordia (East Antarctic plateau) in summer: A strong source from surface snow?, *Atmos. Chem. Phys.*, 14, 9963–9976, doi:10.5194/acp-14-9963-2014, 2014.
- 650 Marbaix, P., Gallée, H., Brasseur, O., and Van Ypersele, J.: *Lateral Boundary Conditions in regional climate models: a detailed study of the relaxation procedure*. *Mon Weather Rev* 131, 461–479, 2003.
- Morcrette, J.-J. : *Assessment of the ECMWF model cloudiness and surface radiation fields at the ARM-SGP site*. *Mon Weather Rev* 130, 257 – 277, 2002.
- 655 Nash, J.E. and Sutcliffe, J.V. : *River flow forecasting through conceptual models part I A discussion of principles*. *J Hydrol* 10 (3), 282 – 290, doi:10.1016/0022-1694(70)90255-6, 1970.
- Pietroni, I., Argentini, S., Petenko, I. : *One Year of Surface-Based Temperature Inversions at Dome C, Antarctica*. *Bound-Lay Meteorol* 150, 131–151, doi: 10.1007/s10546-013-9861-7, 2014.
- 660 Preunkert, S., Legrand, M., Frey, M., Kukui, A., Savarino, J., Gallée, H., King, M., Jourdain, B., Vicars, W., and Helmig, D.: *Formaldehyde (HCHO) in air, snow and interstitial air at Concordia (East Antarctic plateau) in summer*, *Atmos. Chem. Phys. Discuss.*, 14, 32027--32070, doi :10.5194/acpd-14-32027-2014, 2014.

- Sadibekova, T., Fossat, E., Genthon, C., Krinner, G., Aristidi, E., Agabi, K., and Azouit, M. : On the atmosphere for astronomers above Dome C, Antarctica, *Antarctic Science*, 18(3), 437-444, 2006.
- 665 Van Dijk, A., Moen, A., and de Bruin, H. : The principles of surface flux physics : theory, practice and description of the ECPACK library. Internal report 2004/1, Meteorology and Air Quality Group, Wageningen University, Wageningen, The Netherlands, 2006.
- 670 Sukoriansky, S., Galperin, P., and Veniamin P.: Application of a new spectral theory on stably stratified turbulence to the atmospheric boundary layer over sea ice. *Bound-Lay Meteorol* 117, 231 – 257, 2005.
- Swain, M.R., and Gallée, H. : Antarctic Boundary Layer Seeing. *Astr Soc P*, 118, 1190—1197, 2006.
- Van As, D., van den Broeke, M. R. and Helsen, M. M. Structure and dynamics of the summertime atmospheric boundary layer over the Antarctic plateau, I: Measurements and model validation, *J. Geophys. Res.*, 111, D007102, doi:10.1029/2005JD005948, 2006.
- 675 Walden, Von P., Warren, S.G., and Tuttle, E. : Atmospheric Ice Crystals over the Antarctic Plateau in Winter. *J Appl Meteorol* 42: 1391 – 1405, 2003
- Wamser, C. and Lykossov, V.N. : On the Friction Velocity during Blowing Snow, *Beitr. Phys. Atmosph.*, 68: 85 – 94, 1995.
- 680 Wendler, G. and Kelley , J. : On the albedo of snow in Antarctica: a contribution to I.A.G.O., *J. Glaciol.* , 34 (116) : 19 - 25, 1988